Micro-Scale Mapping of Soil Organic Carbon: The Potential of Soft X-Ray Spectromicroscopy

Maoz Dor[1]*, Tom Regier[2], Zachary Arthur[2], Andrey Guber[1], and Alexandra Kravchenko[1]

1. Department of Plant, Soil and Microbial Sciences, Michigan State University, East Lansing, MI, USA
2. Canadian Light Source, University of Saskatchewan, 44 Innovation Boulevard, Saskatoon, SK S7N 2V3, Canada.

*Corresponding author: dormaoz@msu.edu

Abstract

Soil organic carbon (SOC) plays a crucial role in soil fertility, productivity, and global carbon cycling. However, the mechanisms governing SOC persistence and turnover are not fully understood, hindering effective carbon management strategies. Especially limiting are challenges to visualize and characterize spatial distribution patterns of SOC within the intact soil. This study presents a novel approach to map carbon content and composition in intact soil samples using synchrotron X-ray spectromicroscopy at a 4-100 μm resolution. Intact soil cores were collected, fixed with sodium silicate, and polished to create smooth surfaces suitable for soft X-ray analysis. X-ray fluorescence (XRF) maps provided an overview of the total carbon distribution, enabling the identification of carbon-rich regions of interest. Near edge X-ray absorption fine structure (NEXAFS) spectromicroscopy was then employed to obtain spatially resolved carbon speciation data within these regions. This method enabled the analysis of relatively large intact soil cores (16,000 μm Ø and 15,000 μm height), preserving a variety of root and particulate organic matter fragments as well as pores ranging in size from 35 to 850 mm. Spectral fitting using reference standards revealed distinct spatial patterns of aromatic, aliphatic, and carboxylic carbon compounds associated with different soil structural features. Aromatic carbon was enriched around root fragments and the soil matrix, while carboxylic compounds were concentrated at pore-matrix interfaces, suggesting a correlation between soil pore structure and carbon chemical composition. The proposed novel approach provides opportunities for future unprecedented insights into the interplay between pore architecture and organic molecular diversity, the two key factors governing mechanisms of SOC protection and persistence in the soil.

Keywords: soil organic carbon, soil pore architecture, soil C spectromicroscopy, NEXAFS, micro-X-ray fluorescence, carbon speciation

Introduction

Long term preservation of soil carbon, the largest terrestrial carbon pool on earth, has implications for soil fertility, productivity, water flow, gas exchange, and global atmospheric greenhouse gas emissions[1]. Soil pore structure serves as the scaffoldings for soil functioning – the framework in which most physical, biological and chemical processes take place, particularly such processes that contribute to decomposition or protection of soil organic carbon (SOC)[2–5]. The soil functional complexity, derived to a great extent by the spatial heterogeneity of the pore structure, is leading to vast variability in SOC persistence and turnover rates[6,7]. In addition, the effectiveness with which soil microorganisms decompose organic matter plays a role in determining how well carbon is sequestered in the soil[8]. Microbial decomposition is impacted by the microbial community composition, as well as by the physical and hydrological properties of the soil, which regulate the interactions between decomposers and carbon sources. Over the past decade, a growing body of research has recognized the relationship between pore sizes and their functionalities[9]. For example, pores in the size order of tens of microns are optimal as microbial habitats with prevalent decomposition of newly added C, while pores <30 μm are regarded as sites for carbon storage and protection[2,9–11]. Another aspect of carbon protection is the molecular composition of SOC. The molecular diversity of the organic compounds controls the decomposition process. Higher diversity can increase the decomposers' metabolic costs, leading to a greater proportion of persistent carbon compounds[6,12]. Thus, coupling these two aspects: pore structure spatial heterogeneity and organic molecular diversity is crucial for better understanding SOC protection and storage mechanisms.

Currently, chemical characterization of SOC persistence [6,7,13,14] and spatial heterogeneity of C composition at the mineral-SOC interface[15–17] are explored either in disturbed bulk soils or at the nanometer scale. For example, nano-scale secondary ion mass spectrometry (NanoSIMS) was successfully used to map the soil organic-mineral complexes and the soil-root interfaces [16,18,19]. Moreover, techniques like Fourier-transform infrared (FTIR) spectromicroscopy[20,21] and scanning transmission X-ray spectromicroscopy (STXM)[17,22], both in transmission mode requiring thin sectioning, have also been reported to successfully mapping of organic compounds at the organic-soil interface to characterize mineral associated organic matter (MAOM). Considering the pervasiveness of soil heterogeneity at all spatial scales, it is crucial to analyze SOC within its natural context, i.e. intact samples. Moreover, modeling and predicting soil carbon processing requires addressing the influence of soil physical environment, as represented by the pore structure, at the scales relevant for SOC input from plant roots, its subsequent microbial processing, and protection. However, the lack of suitable measuring approaches currently limits the ability to quantify the effect of soil pore structure on SOC chemical composition. Recent advancements and accessibility of X-ray microtomography have enabled the well-established visualization and quantification of intact soil structures[2,3,8,23]. However, spatially resolving and co-localizing soil structural features with carbon content and speciation with hard x-rays remains elusive due to their low photon interaction cross section with light elements. We present here a new approach to map carbon chemistry for large, intact soil samples using synchrotron soft X-ray fluorescence (XRF) spectromicroscopy and microspectroscopy techniques.

Methods

Sample preparation

The studied soil was a silty loam Ultisol from a permanent pasture located at the USDA-ARS Farming Systems Project long-term field trial in Beltsville Maryland. The soil texture was 23.8% sand, 59.6% silt, and 16.7% clay, with 1.3% SOC. Intact soil cores (5 cm Ø) were collected from 5-10 cm depth. The cores were then sub-sampled into polycarbonate cylinders (16,000 μm Ø and 15,000 μm height), hereafter, cores (Fig. 1a).

The spectromicroscopy measurements are best performed on flat surfaces to avoid artifacts stemming from the short penetration depth of soft x-rays. Therefore, the cores were fixed with sodium silicate (30%) (Radnor, PA, USA) and subsequently polished to create smooth surfaces. Sodium silicate was chosen for fixation due to its low viscosity, which facilitates sample infiltration, and to avoid introducing additional carbon to the soil. It is used as a soil stabilizer[24] as well as a binder for sand foundry[25] due to its ability to solidify mainly through dehydration or reaction with atmospheric carbon dioxide to form silica-gel. The cores were initially embedded in sodium silicate using a two-step process. First, saturation was achieved from the bottom until the core surface appeared wet (~15 min). Then, the cores were completely submerged and placed under a vacuum of -40 kPa overnight. This step removed air from the soil pores. Once ambient pressure was restored, the sodium silicate penetrated the pores and subsequently cured for 5 days at 40°C. As water evaporates from the sodium silicate solution, it becomes more concentrated and eventually solidifies into a glassy substance[25]. Finally, the cores were polished with a series of polishing papers.

Spectromicroscopy and near edge X-ray adsorption fine structure (NEXAFS)spectroscopy

X-ray maps and spectroscopy data acquisition was carried at the spherical grating monochromator (SGM) beamline at the Canadian Light Source (Saskatoon, SK). A silicon drift detector (Amptek Fast SDD), positioned at 90^{o} to the incident beam in the plane of polarization to minimize scattering, was used to collect the C partial fluorescence yield (PFY) of the sample with an energy resolution of around 100 eV. A measurement of the B PFY for pure Boron Nitride was used to correct for changes in the incident beam intensity by dividing the raw C PFY by the boron PFY. Energy calibration was confirmed using a the C1s (C=O) to π* transition at 288.7 eV of a citric acid standard[26].

A map of the soil carbon content of the soil core surface was assessed by a X-ray fluorescence (XRF) map made with an excitation energy of 320 eV (above the C K-edge) with 35 μm resolution (Fig. 1b). The XRF carbon map coupled with light microscopy image of the surface was used to find a region of interest that will include a C 'hotspot'. Next, a XRF stack of 60 individual maps acquired with incident photon between 282-294 eV (0.2 eV step size) was collected, capturing the C K-edge spectral data for every pixel (**Fig. 1**c). In Addition, NEXAFS spectra from pressed pellets of organic compounds references were collected. 15 individual 60 s slew scans were collected at

different positions on each sample and combined to create the NEXAFS measurement for that reference compound. The references represented aromatic, aliphatic and carboxylic acid compounds of plant and microorganisms' origin prevalent in soils[26–28] and included tanic acid, starch, and malic acid. Linear combination fitting using these three reference spectra was calculated for each pixel in the spectromicroscopy stacks. All data visualization and analysis was performed in Python (ver. 3.9) using numpy[29], scipy[30], and scikit-learn[31] libraries.

Results and Discussion

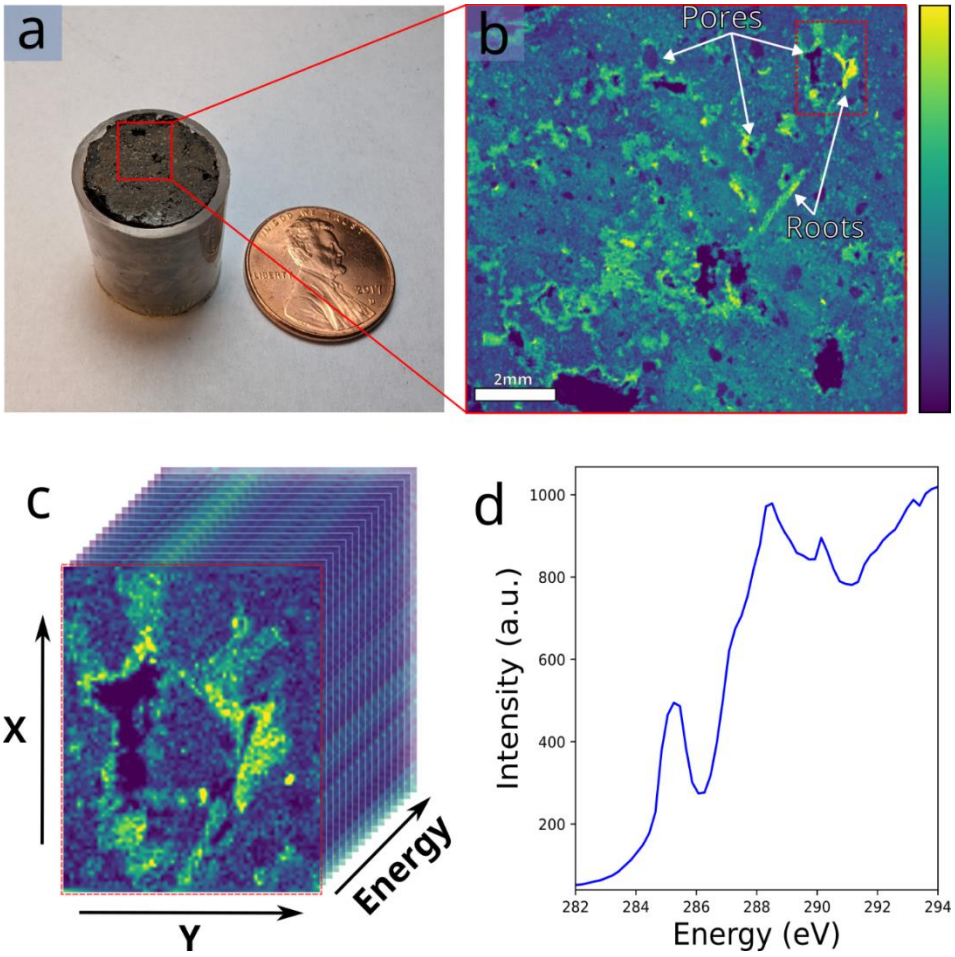

Fig. 1. Workflow for carbon mapping and spectromicroscopy in soil samples. (a) soil core. (b) XRF map acquired at 320 eV above the C K-edge to map total carbon in the sample and identify regions of interest (marked with red dashed rectangle) for spectromicroscopy stack acquisition. (c) Spectromicroscopy stack of 60 XRF maps acquired across the C K-edge (282-294 eV) with 0.2 eV step size. (d) Spectral data representing the sum of partial fluorescence yield from all partial fluorescence measurements of the stack, used for carbon compound speciation.

The workflow for micro-scale mapping of soil organic carbon at 35 µm resolution is presented in Fig. 1. The carbon-free fixation agent, sodium silicate, are able to successfully preserve the

structure of the soil core. This allowed polishing the surface to minimize roughness, a common issue with soil samples that can lead to shadowing and edge effect artifacts during soft X-ray analysis. Moreover, the developed sample preparation method enabled us to work with a relatively large intact soil core (16,000 μm Ø and 15,000 μm height) (Fig. 1a), where a variety of root and particulate organic matter fragments as well as a variety of pores ranging in size from 35 to 850 μm were present on the exposed measured surface (Fig. 1a). To our knowledge, intact imaging of soil cores of this size range was previously achievable only with carbon-based resins[15], while only much smaller samples (<500 μm Ø) could be non-destructively imaged through thin sectioning techniques [20,22].

The total carbon content XRF map acquired at 320 eV (Fig. 1b) demonstrated good contrast and clearly delineated carbon rich features in the image (e.g. roots). Due to the relatively short acquisition time (~60 min), these maps are ideal for identifying regions of interest for further investigation using techniques requiring longer times, such as high-resolution carbon maps (achievable up to ~4 μm in our current setup) and/or spectromicroscopy.

In Fig. 2 we present the results of the XRF spectromicroscopy stack acquired for an area (~3.3×10^6 μm^2) surrounding a carbon-rich root fragment which not only produced a good contrast between different soil components (pores, root, soil matrix), but also depicted variations in spectral information within different regions of interests (Fig. 2). As expected, low intensity C signal was found in soil pores, or in carbon-deficient areas. The spectra measured for the root area shows peaks at 285.3, 287, and 288.4 eV associated with aromatic, aliphatic and carboxylic carbon moieties[28,32]. Interestingly, the soil matrix in the vicinity of the pores exhibited higher overall carbon content, despite showing a relatively similar spectral composition to other soil matrix regions. Additionally, a peak at 290.1 eV associated with carbonate moiety[32] was present in the soil matrix regions. The demonstrated ability to visualize the spatial distribution of these species and compounds is particularly intriguing since they play a significant role in carbon protection and persistence[2,6].

In Fig. 3, we demonstrate a procedure for fitting reference organic compounds to the spectromicroscopy stack using linear combinations to obtain compositional maps. By fitting NEXAFS spectra references to the spectromicroscopy stack data, we observed internal contrast within the map, revealing regions with distinct chemical composition (Fig. 3).

Analysis of the different compositional maps (Fig. 3c) reveals a high concentration of aromatic carbon around the root and soil matrix, particularly in the vicinity of the pores. Additionally, a high concentration of aliphatic compounds is observed mainly in the root area, while the pore-matrix interface exhibits a higher concentration of carboxylic compounds. This spatial distribution suggests a correlation between the soil structure and the distribution of carbon compounds. The root acts as a primary carbon source. Pores facilitate microbial decomposition[2], which explains the high concentration of carboxylic compounds around the pore interface. Finally, the soil matrix serves as a carbon sink, containing more complex, aromatic carbon compounds.

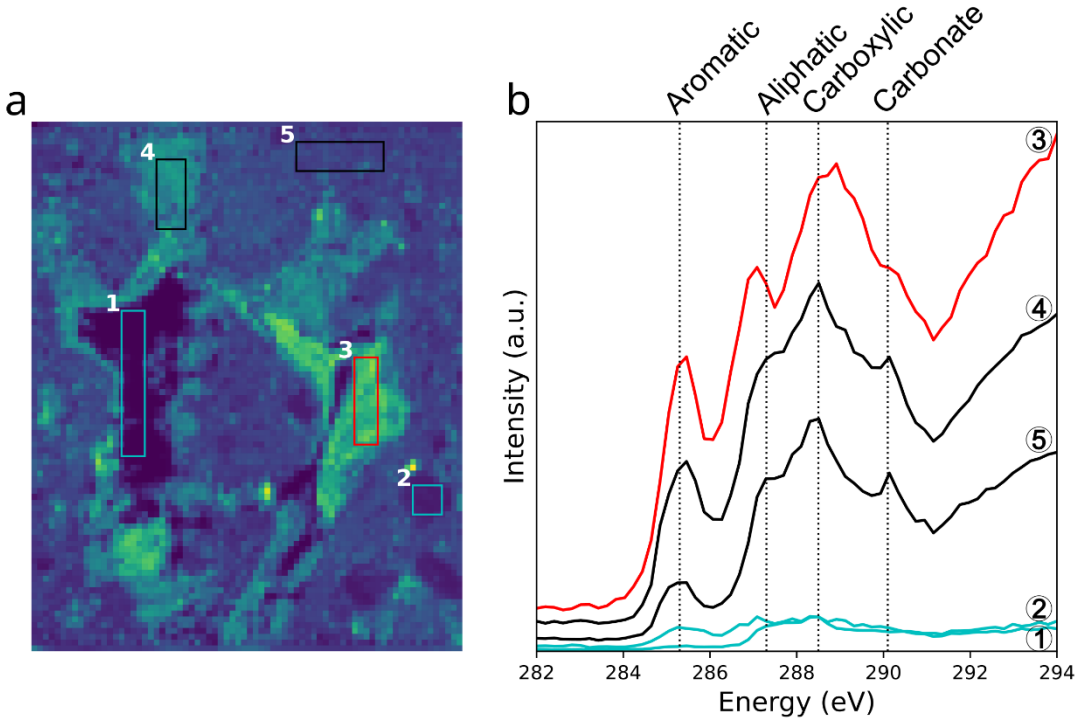

Fig. 2. Selected regions of interests of different soil phases, marked with rectangles (1-2 pores, 3 root fragment, 4-5 soil matrix), on a carbon content map (a) comprising different levels of carbon content, and their respective spectral data (b) which allows to spatially resolve C spectral information. Dash lines marks (from left to right) energies associated with aromatic (285.3 eV), aliphatic (287.3 eV), carboxylic (288.4 eV), and carbonate (290.1 eV) carbon moieties.

This short communication presents a proof of concept for a new approach to 2D mapping of carbon contents and compositions on surfaces of landscape scale relevant, intact soil samples. The information obtained using the proposed approach can be combined with other spatially resolved techniques (e.g., x-ray tomography, zymography, electron microscopy), shedding light on and furthering our understanding of carbon sequestration and storage mechanisms. By integrating spatially-resolved structural and chemical information from intact samples, this work paves the way for a more comprehensive and quantitative understanding of carbon dynamics in soils, with potential implications for soil carbon management and climate change mitigation strategies.

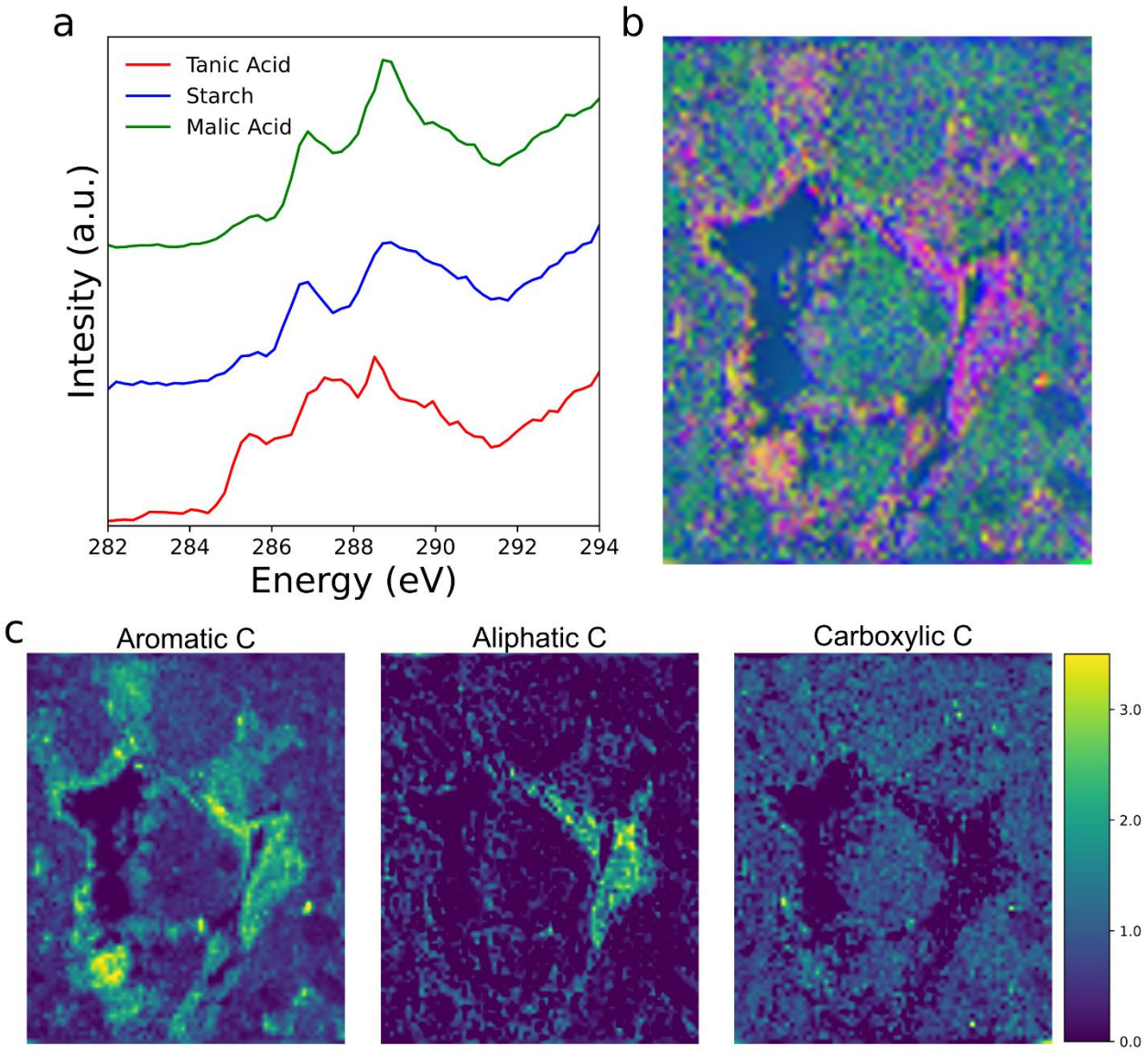

Fig. 3. Mapping carbon composition of an intact soil sample surface. (a) reference standard NEXAFS spectra of aromatic, aliphatic and carboxylic compounds. (b) composite image of aromatic (red), aliphatic (blue), and carboxylic (green) carbon following a linear combination fit, and the separate compositional maps channels (c).

References

(1) Friedlingstein, P.; Jones, M. W.; O'Sullivan, M.; Andrew, R. M.; Bakker, D. C. E.; Hauck, J.; Le Quéré, C.; Peters, G. P.; Peters, W.; Pongratz, J.; Sitch, S.; Canadell, J. G.; Ciais, P.; Jackson, R. B.; Alin, S. R.; Anthoni, P.; Bates, N. R.; Becker, M.; Bellouin, N.; Bopp, L.; Chau, T. T. T.; Chevallier, F.; Chini, L. P.; Cronin, M.; Currie, K. I.; Decharme, B.; Djeutchouang, L. M.; Dou, X.; Evans, W.; Feely, R. A.; Feng, L.; Gasser, T.; Gilfillan, D.; Gkritzalis, T.; Grassi, G.; Gregor,

L.; Gruber, N.; Gürses, Ö.; Harris, I.; Houghton, R. A.; Hurtt, G. C.; Iida, Y.; Ilyina, T.; Luijkx, I. T.; Jain, A.; Jones, S. D.; Kato, E.; Kennedy, D.; Klein Goldewijk, K.; Knauer, J.; Korsbakken, J. I.; Körtzinger, A.; Landschützer, P.; Lauvset, S. K.; Lefèvre, N.; Lienert, S.; Liu, J.; Marland, G.; McGuire, P. C.; Melton, J. R.; Munro, D. R.; Nabel, J. E. M. S.; Nakaoka, S.-I.; Niwa, Y.; Ono, T.; Pierrot, D.; Poulter, B.; Rehder, G.; Resplandy, L.; Robertson, E.; Rödenbeck, C.; Rosan, T. M.; Schwinger, J.; Schwingshackl, C.; Séférian, R.; Sutton, A. J.; Sweeney, C.; Tanhua, T.; Tans, P. P.; Tian, H.; Tilbrook, B.; Tubiello, F.; van der Werf, G. R.; Vuichard, N.; Wada, C.; Wanninkhof, R.; Watson, A. J.; Willis, D.; Wiltshire, A. J.; Yuan, W.; Yue, C.; Yue, X.; Zaehle, S.; Zeng, J. Global Carbon Budget 2021. *Earth System Science Data* **2022**, *14* (4), 1917–2005. https://doi.org/10.5194/essd-14-1917-2022.

(2) Kravchenko, A. N.; Guber, A. K.; Razavi, B. S.; Koestel, J.; Quigley, M. Y.; Robertson, G. P.; Kuzyakov, Y. Microbial Spatial Footprint as a Driver of Soil Carbon Stabilization. *Nature Communications* **2019**, *10* (1), 3121. https://doi.org/10.1038/s41467-019-11057-4.

(3) Vogel, H.-J.; Balseiro-Romero, M.; Kravchenko, A.; Otten, W.; Pot, V.; Schlüter, S.; Weller, U.; Baveye, P. C. A Holistic Perspective on Soil Architecture Is Needed as a Key to Soil Functions. *European Journal of Soil Science* **2022**, *73* (1), e13152. https://doi.org/10.1111/ejss.13152.

(4) Tiedje, J. M.; Cho, J. C.; Murray, A.; Treves, D.; Xia, B.; Zhou, J. Soil Teeming with Life: New Frontiers for Soil Science. *Sustainable management of soil organic matter* **2001**, 393–425. https://doi.org/10.1079/9780851994659.0393.

(5) Carson, J. K.; Gonzalez-Quiñones, V.; Murphy, D. V.; Hinz, C.; Shaw, J. A.; Gleeson, D. B. Low Pore Connectivity Increases Bacterial Diversity in Soil. *Applied and Environmental Microbiology* **2010**, *76* (12), 3936–3942. https://doi.org/10.1128/AEM.03085-09.

(6) Lehmann, J.; Hansel, C. M.; Kaiser, C.; Kleber, M.; Maher, K.; Manzoni, S.; Nunan, N.; Reichstein, M.; Schimel, J. P.; Torn, M. S.; Wieder, W. R.; Kögel-Knabner, I. Persistence of Soil Organic Carbon Caused by Functional Complexity. *Nature Geoscience* **2020**, *13* (8), 529–534. https://doi.org/10.1038/s41561-020-0612-3.

(7) Schmidt, M. W. I.; Torn, M. S.; Abiven, S.; Dittmar, T.; Guggenberger, G.; Janssens, I. A.; Kleber, M.; Kögel-Knabner, I.; Lehmann, J.; Manning, D. A. C.; Nannipieri, P.; Rasse, D. P.; Weiner, S.; Trumbore, S. E. Persistence of Soil Organic Matter as an Ecosystem Property. *Nature* **2011**, *478* (7367), 49–56. https://doi.org/10.1038/nature10386.

(8) Baveye, P. C.; Otten, W.; Kravchenko, A.; Balseiro-Romero, M.; Beckers, É.; Chalhoub, M.; Darnault, C.; Eickhorst, T.; Garnier, P.; Hapca, S.; Kiranyaz, S.; Monga, O.; Mueller, C. W.; Nunan, N.; Pot, V.; Schlüter, S.; Schmidt, H.; Vogel, H. J. Emergent Properties of Microbial Activity in Heterogeneous Soil Microenvironments: Different Research Approaches Are Slowly Converging, yet Major Challenges Remain. *Frontiers in Microbiology* **2018**, *9* (AUG), 1929. https://doi.org/10.3389/FMICB.2018.01929/BIBTEX.

(9) Franklin, S. M.; Kravchenko, A. N.; Vargas, R.; Vasilas, B.; Fuhrmann, J. J.; Jin, Y. The Unexplored Role of Preferential Flow in Soil Carbon Dynamics. *Soil Biology and Biochemistry* **2021**, *161*, 108398. https://doi.org/10.1016/j.soilbio.2021.108398.

(10) Kravchenko, A. N.; Guber, A. K.; Razavi, B. S.; Koestel, J.; Blagodatskaya, E. V.; Kuzyakov, Y. Spatial Patterns of Extracellular Enzymes: Combining X-Ray Computed Micro-Tomography and 2D Zymography. *Soil Biology and Biochemistry* **2019**, *135*, 411–419. https://doi.org/10.1016/j.soilbio.2019.06.002.

(11) Yao, S.-H.; Zhang, B.; Hu, F. Soil Biophysical Controls over Rice Straw Decomposition and Sequestration in Soil: The Effects of Drying Intensity and Frequency of Drying and Wetting Cycles. *Soil Biology and Biochemistry* **2011**, *43* (3), 590–599. https://doi.org/10.1016/j.soilbio.2010.11.027.

(12) Lane, N.; Martin, W. The Energetics of Genome Complexity. *Nature* **2010**, *467* (7318), 929–934. https://doi.org/10.1038/nature09486.

(13) Weng, Z. (Han); Lehmann, J.; Van Zwieten, L.; Joseph, S.; Archanjo, B. S.; Cowie, B.; Thomsen, L.; Tobin, M. J.; Vongsvivut, J.; Klein, A.; Doolette, C. L.; Hou, H.; Mueller, C. W.; Lombi, E.; Kopittke, P. M. Probing the Nature of Soil Organic Matter. *Critical Reviews in Environmental Science and Technology* **2022**, *52* (22), 4072–4093. https://doi.org/10.1080/10643389.2021.1980346.

(14) Lavallee, J. M.; Soong, J. L.; Cotrufo, M. F. Conceptualizing Soil Organic Matter into Particulate and Mineral-Associated Forms to Address Global Change in the 21st Century. *Global Change Biology* **2020**, *26* (1), 261–273. https://doi.org/10.1111/gcb.14859.

(15) Lippold, E.; Schlüter, S.; Mueller, C. W.; Höschen, C.; Harrington, G.; Kilian, R.; Gocke, M. I.; Lehndorff, E.; Mikutta, R.; Vetterlein, D. Correlative Imaging of the Rhizosphere─A Multimethod Workflow for Targeted Mapping of Chemical Gradients. *Environ. Sci. Technol.* **2023**, *57* (3), 1538–1549. https://doi.org/10.1021/acs.est.2c07340.

(16) Witzgall, K.; Vidal, A.; Schubert, D. I.; Höschen, C.; Schweizer, S. A.; Buegger, F.; Pouteau, V.; Chenu, C.; Mueller, C. W. Particulate Organic Matter as a Functional Soil Component for Persistent Soil Organic Carbon. *Nat Commun* **2021**, *12* (1), 4115. https://doi.org/10.1038/s41467-021-24192-8.

(17) Lehmann, J.; Solomon, D.; Kinyangi, J.; Dathe, L.; Wirick, S.; Jacobsen, C. Spatial Complexity of Soil Organic Matter Forms at Nanometre Scales. *Nature Geosci* **2008**, *1* (4), 238–242. https://doi.org/10.1038/ngeo155.

(18) Clode, P. L.; Kilburn, M. R.; Jones, D. L.; Stockdale, E. A.; Cliff, J. B., III; Herrmann, A. M.; Murphy, D. V. In Situ Mapping of Nutrient Uptake in the Rhizosphere Using Nanoscale Secondary Ion Mass Spectrometry. *Plant Physiology* **2009**, *151* (4), 1751–1757. https://doi.org/10.1104/pp.109.141499.

(19) Li, Q.; Chang, J.; Li, L.; Lin, X.; Li, Y. Research Progress of Nano-Scale Secondary Ion Mass Spectrometry (NanoSIMS) in Soil Science: Evolution, Applications, and Challenges. *Science of The Total Environment* **2023**, *905*, 167257. https://doi.org/10.1016/j.scitotenv.2023.167257.

(20) Shabtai, I. A.; Wilhelm, R. C.; Schweizer, S. A.; Höschen, C.; Buckley, D. H.; Lehmann, J. Calcium Promotes Persistent Soil Organic Matter by Altering Microbial Transformation of Plant Litter. *Nat Commun* **2023**, *14* (1), 6609. https://doi.org/10.1038/s41467-023-42291-6.

(21) Lehmann, J.; Kinyangi, J.; Solomon, D. Organic Matter Stabilization in Soil Microaggregates: Implications from Spatial Heterogeneity of Organic Carbon Contents and Carbon Forms. *Biogeochemistry* **2007**, *85* (1), 45–57. https://doi.org/10.1007/s10533-007-9105-3.

(22) Weng, Z. (Han); Van Zwieten, L.; Tavakkoli, E.; Rose, M. T.; Singh, B. P.; Joseph, S.; Macdonald, L. M.; Kimber, S.; Morris, S.; Rose, T. J.; Archanjo, B. S.; Tang, C.; Franks, A. E.; Diao, H.; Schweizer, S.; Tobin, M. J.; Klein, A. R.; Vongsvivut, J.; Chang, S. L. Y.; Kopittke, P. M.; Cowie, A. Microspectroscopic Visualization of How Biochar Lifts the Soil Organic Carbon Ceiling. *Nat Commun* **2022**, *13* (1), 5177. https://doi.org/10.1038/s41467-022-32819-7.

(23) Schlüter, S.; Sammartino, S.; Koestel, J. Exploring the Relationship between Soil Structure and Soil Functions via Pore-Scale Imaging. *Geoderma* **2020**, *370*, 114370. https://doi.org/10.1016/j.geoderma.2020.114370.

(24) Koohestani, B.; Darban, A. K.; Mokhtari, P.; Darezereshki, E.; Yilmaz, E. Geopolymerization of Soil by Sodium Silicate as an Approach to Control Wind Erosion. *Int. J. Environ. Sci. Technol.* **2021**, *18* (7), 1837–1848. https://doi.org/10.1007/s13762-020-02943-2.

(25) Owusu, Y. A. Physical-Chemistry Study of Sodium Silicate as a Foundry Sand Binder. *Advances in Colloid and Interface Science* **1982**, *18* (1), 57–91. https://doi.org/10.1016/0001-8686(82)85031-8.

(26) Solomon, D.; Lehmann, J.; Kinyangi, J.; Liang, B.; Heymann, K.; Dathe, L.; Hanley, K.; Wirick, S.; Jacobsen, C. Carbon (1s) NEXAFS Spectroscopy of Biogeochemically Relevant Reference Organic Compounds. *Soil Science Society of America Journal* **2009**, *73* (6), 1817–1830. https://doi.org/10.2136/sssaj2008.0228.

(27) *Introduction of Soft X-Ray Spectromicroscopy as an Advanced Technique for Plant Biopolymers Research | PLOS ONE*. https://journals.plos.org/plosone/article?id=10.1371/journal.pone.0122959 (accessed 2024-05-20).

(28) Solomon, D.; Lehmann, J.; Kinyangi, J.; Liang, B.; Schäfer, T. Carbon K-Edge NEXAFS and FTIR-ATR Spectroscopic Investigation of Organic Carbon Speciation in Soils. *Soil Sci. Soc. Am. j.* **2005**, *69* (1), 107–119. https://doi.org/10.2136/sssaj2005.0107dup.

(29) Harris, C. R.; Millman, K. J.; van der Walt, S. J.; Gommers, R.; Virtanen, P.; Cournapeau, D.; Wieser, E.; Taylor, J.; Berg, S.; Smith, N. J.; Kern, R.; Picus, M.; Hoyer, S.; van Kerkwijk, M. H.; Brett, M.; Haldane, A.; del Río, J. F.; Wiebe, M.; Peterson, P.; Gérard-Marchant, P.; Sheppard, K.; Reddy, T.; Weckesser, W.; Abbasi, H.; Gohlke, C.; Oliphant, T. E. Array Programming with NumPy. *Nature* **2020**, *585* (7825), 357–362. https://doi.org/10.1038/s41586-020-2649-2.

(30) Virtanen, P.; Gommers, R.; Oliphant, T. E.; Haberland, M.; Reddy, T.; Cournapeau, D.; Burovski, E.; Peterson, P.; Weckesser, W.; Bright, J.; Walt, S. J. van der; Brett, M.; Wilson, J.; Millman, K. J.; Mayorov, N.; Nelson, A. R. J.; Jones, E.; Kern, R.; Larson, E.; Carey, C. J.; Polat, İ.; Feng, Y.; Moore, E. W.; VanderPlas, J.; Laxalde, D.; Perktold, J.; Cimrman, R.; Henriksen, I.; Quintero, E. A.; Harris, C. R.; Archibald, A. M.; Ribeiro, A. H.; Pedregosa, F.; Mulbregt, P. van; Vijaykumar, A.; Bardelli, A. P.; Rothberg, A.; Hilboll, A.; Kloeckner, A.; Scopatz, A.; Lee, A.; Rokem, A.; Woods, C. N.; Fulton, C.; Masson, C.; Häggström, C.; Fitzgerald, C.; Nicholson, D. A.; Hagen, D. R.; Pasechnik, D. V.; Olivetti, E.; Martin, E.; Wieser, E.; Silva, F.; Lenders, F.; Wilhelm, F.; Young, G.; Price, G. A.; Ingold, G. L.; Allen, G. E.; Lee, G. R.; Audren, H.; Probst, I.; Dietrich, J. P.; Silterra, J.; Webber, J. T.; Slavič, J.; Nothman, J.; Buchner, J.; Kulick, J.; Schönberger, J. L.; Cardoso, J. V. de M.; Reimer, J.; Harrington, J.; Rodríguez, J. L. C.; Nunez-Iglesias, J.; Kuczynski, J.; Tritz, K.; Thoma, M.; Newville, M.; Kümmerer, M.; Bolingbroke, M.; Tartre, M.; Pak, M.; Smith, N. J.; Nowaczyk, N.; Shebanov, N.; Pavlyk, O.; Brodtkorb, P. A.; Lee, P.; McGibbon, R. T.; Feldbauer, R.; Lewis, S.; Tygier, S.; Sievert, S.; Vigna, S.; Peterson, S.; More, S.; Pudlik, T.; Oshima, T.; Pingel, T. J.; Robitaille, T. P.; Spura, T.; Jones, T. R.; Cera, T.; Leslie, T.; Zito, T.; Krauss, T.; Upadhyay, U.; Halchenko, Y. O.; Vázquez-Baeza, Y. SciPy 1.0: Fundamental Algorithms for Scientific Computing in Python. *Nature Methods 2020 17:3* **2020**, *17* (3), 261–272. https://doi.org/10.1038/s41592-019-0686-2.

(31) Pedregosa, F.; Varoquaux, G.; Gramfort, A.; Michel, V.; Thirion, B.; Grisel, O.; Blondel, M.; Prettenhofer, P.; Weiss, R.; Dubourg, V.; Vanderplas, J.; Passos, A.; Cournapeau, D. Scikit-Learn: Machine Learning in Python. *MACHINE LEARNING IN PYTHON* **2011**, *12*, 2825–2830.

(32) Lutfalla, S.; Barré, P.; Bernard, S.; Le Guillou, C.; Alléon, J.; Chenu, C. Multidecadal Persistence of Organic Matter in Soils: Multiscale Investigations down to the Submicron Scale. *Biogeosciences* **2019**, *16* (7), 1401–1410. https://doi.org/10.5194/bg-16-1401-2019.